In vivo imaging rhodopsin distribution in the photoreceptors with nano-second pulsed scanning laser ophthalmoscopy

Tan Liu[1], Xiaojing Liu[1], Rong Wen[2], Byron L. Lam[2], Shuliang Jiao[1]

[1]Department of Biomedical Engineering, Florida International University, Miami, FL 33174, USA; [2]Bascom Palmer Eye Institute, Miller School of Medicine, University of Miami, Miami, FL 33136, USA

Correspondence to: Shuliang Jiao. 10555 W Flagler St, EC 2610, Department of Biomedical Engineering, Florida International University, Miami, FL 33174, USA. Email: shjiao@fiu.edu.

Background: Rhodopsin is a biomarker for the function of rod photoreceptors, the dysfunction of which is related to many blinding diseases like retinitis pigmentosa and age-related macular degeneration. Imaging rhodopsin quantitatively may provide a powerful clinical tool for diagnosis of these diseases. To map rhodopsin distribution accurately in the retina, absorption by rhodopsin intermediates need to be minimized.

Methods and materials: We developed nano-second pulsed scanning laser ophthalmoscopy (SLO) to image rhodopsin distribution in the retina. The system takes advantage of the light-induced shift of rhodopsin absorption spectra, which in turn affects the fundus spectral reflection before and after photobleaching. By imaging the retina twice, one in the dark-adapted state and the other one in the light-adapted state, the rhodopsin absorption change can be calculated from the differential image, which is a function of the rhodopsin concentration in the rod photoreceptors.

Results: The system was successfully applied to *in vivo* imaging of rat retina in different bleaching conditions to verify its feasibility. Our studies showed that the differential image between the dark- and light-adapted states represents rhodopsin distribution in the retina. We also conducted a dynamic bleaching experiment to prove the importance of reducing light absorption of rhodopsin intermediates.

Conclusions: The preliminary results showed that our nano-second pulsed-light SLO is promising in imaging the functional biomarker of the rod photoreceptors. By using nanosecond pulsed laser, in which one laser pulse generates one pixel of the image, the absorption of rhodopsin intermediates can be reduced.

Keywords: Densitometry; optical reflectometry; photoreceptors; rhodopsin; scanning laser ophthalmoscopy (SLO)

Introduction

Rhodopsin is the photopigment in vertebrate rod photoreceptors. Visual phototransduction is initiated when rhodopsin absorbs a photon and the rhodopsin photo-cycle is activated. Rhodopsin (absorption peak: 500 nm) is photoisomerized in an ultrafast time scale (~200 fs) (1) and then proceeds with the photo-cycle through a series of well characterized intermediates. The full photo-cycle takes minutes before rhodopsin is regenerated, starting from the intermediate state of photo-rhodopsin and ending at the intermediate state of metarhodopsin III. The peak absorption first red shifts to 570 nm upon photo isomerization in about 200 fs, then blue shifts to 450 nm when the intermediate changes to the form of metarhodopsin III (2,3). Rhodopsin is thus a functional biomarker of photoreceptors, and the light-induced shift in absorption spectrum can be used to assess the function of rod photoreceptors. As a result, quantitatively mapping the density distribution of rhodopsin is able to image the function of the rod photoreceptors.

The traditional techniques for imaging the distribution

Table 1 Summary of absorption peak wavelength and photoisomerization time scale which are corresponding to rhodopsin and all intermediates (3)

Short name of intermediates	Rhodopsin	Photo-	Batho-	BSI	Lumi-	Meta-I	Meta-II	Meta-III
Absorption peak (nm)	500	570	543	477	497	480	380	450
Time scale (from last intermediate)	0	200 fs	3 ps	ns	ns	µs	ms	min

Photo-, photorhodopsin; Batho-, bathorhodopsin; Lumi-, lumirhodopsin; Meta-I, metarhodopsin I; Meta-II, metarhodopsin II; Meta-III, metarhodopsin III.
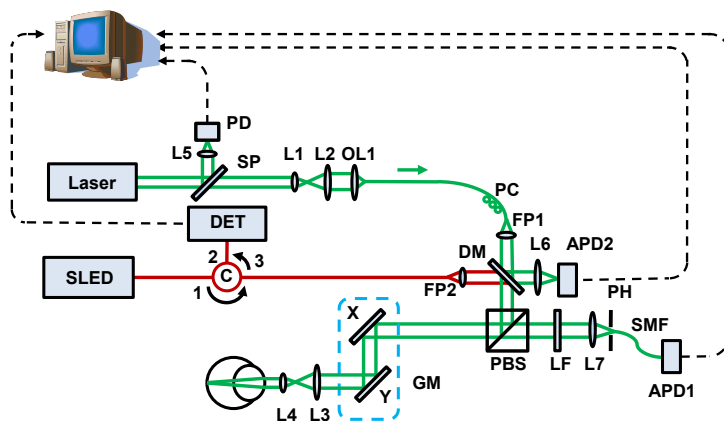

Figure 1 Schematic of the nano-second pulsed scanning laser ophthalmoscopy (SLO). PD, photo-diode; SLED, superluminscent diode; C, circulator; SP, sampler reflector; L1-L7, lens; OL1-2, objective lens; PC, polarization controller; FP1-2, fiber port; DM, dichroic mirror; PBS, polarizing beam splitter cube; GM, galvanometer; LF, laserline filter; PH, pinhole; SMF, single mode fiber; APD1-2, avalanche photodiode; DET, near-infrared detector.

of rhodopsin use a method known as retinal densitometry (4-6), a technique based on optical reflectometry. All the imaging techniques, including fundus photography (7-9) and scanning laser ophthalmoscopy (SLO) (10-12), take advantage of the rhodopsin absorption spectral shift upon photo bleaching, i.e., by measuring the intensity changes of visible light within the rhodopsin absorption spectrum reflected from the retina between the dark- and light-adapted states (13). To calculate rhodopsin concentration accurately, light absorption by the rhodopsin intermediates activated by the probing light should be minimized. In fundus photography the duration of the flash light is usually in the millisecond level. Conventional SLO uses a continuous wave (CW) light source. The exposure time of each pixel of a full frame fundus image is inversely proportional to the scanning speed and is typically in the microsecond level. The optical density calculated from both of these images can be affected significantly by the absorption of rhodopsin intermediates.

The goal of this project is to develop a SLO system using a pulsed laser to reduce the effect of absorption

from rhodopsin intermediates. The system will provide a better platform for rhodopsin imaging and help develop a quantitative model to calculate rhodopsin concentration in the rod photoreceptors. *Table 1* shows the time and absorption information of the rhodopsin photo-cycle. From the table we can see that the first two intermediates are generated in picosecond level and the third intermediate is generated in nanosecond level. Since femtosecond and picosecond pulsed light source are not suitable for our applications due to laser safety concern, we adopted a nanosecond pulsed laser for the project. In this paper, we report on our study on rhodopsin imaging in living animals with a nano-second pulsed scanning laser ophthalmoscope.

Methods and materials

Experimental system

A schematic of the imaging system is shown in *Figure 1*. The system consists of two SLO subsystems, one of which works in the near infrared (NIR) for guiding the alignment process

and the other one works in the visible (VIS) for rhodopsin imaging. A frequency-doubled Nd:YAG laser (SPOT-10-200-532, Elforlight Ltd, UK; output wavelength: 532 nm; maximum pulse energy: 20 µJ; pulse duration: 2 ns; maximum pulse repetition rate: 30 kHz) was used as the illumination light source of the VIS-SLO. The laser light first passed through an uncoated glass plate, the surface reflection from which was focused on a photodiode, the output of which was used to trigger the digitizer for data acquisition. The laser beam was expanded by a beam expander consisting of a lens pair and then coupled into a single mode optical fiber (460 HP, Thorlabs). The light output from the fiber was collimated by a fiber port (PAF-X-11-A, Thorlabs) and merged with the NIR probing light (center wavelength: 840 nm, FWHM bandwidth: 50 nm) by a dichroic mirror. The NIR light came from a superluminescent diode (SLD-37-HP, Superlum, Russia) after passing through a circulator. The combined light was split by a polarizing beam splitter cube (PBS, PBS251, Thorlabs). The vertically polarized components were reflected by the PBS, scanned by an x-y galvanometer (6215H, Cambridge) scanner, and then delivered into the eye by the combination of a relay lens and an ocular lens. A fiber polarization controller was used to optimize the polarization state of the laser output from the fiber, so that the vertical polarization component will dominate and the laser light was delivered to the eye efficiently. The VIS light pulse energy was controlled to be 1.5 nJ/pulse before entering the eye, which is only 4% of our previous calculated safety limit (14), while the NIR light was about 600 µW.

The back-traveling photons reflected from the retina exit the eye with modified polarization states caused by both light scattering and the birefringence of the eye. After passing the PBS, a large portion of the NIR light was reflected into the same delivery path and detected by a photodetector (V-600, Optiphase) at the second port of the circulator. The output of the photodetector was digitized by a high speed digitizer (8 bits, PCI-5154, National Instruments). The horizontally polarized components of the back-reflected VIS light transmitted through the PBS. After passing through a 532 nm laser-line filter (532BP10, Omega) the light was focused onto a 20 µm pinhole, coupled into a single-mode fiber closely placed after the pinhole, and then detected by an avalanche photodiode (APD, APD110A, Thorlabs). An identical APD detected a focused sampling beam reflected from the dichroic mirror for VIS laser power compensation. The outputs of the APDs were simultaneously recorded by the two channels of the digitizer at a sampling rate of 1 GS/s.

Each laser pulse was recorded by 200 samples corresponding to a period of 200 ns.

Animal preparation

We imaged albino rats (Sprague Dawley, 300-500 g, Harlan Laboratories) in the study. The rats were dark-adapted for four hours (15) before the experiment. The rats were anesthetized by intra-peritoneal injection of a cocktail containing ketamine (54 mg/kg body weight) and xylazine (6 mg/kg body weight). We then dilated the rats' pupil with 0.5% tropicamide ophthalmic solution and paralyzed the iris sphincter muscle with 0.5% proparacaine hydrochloride ophthalmic solution. After sedated, a powerless contact lens was put on the eye to prevent cornea dehydration and cataract formation (16). All experiments were performed in compliance with the ARVO Statement for the Use of Animals in Ophthalmic and Vision Research, and with the guidelines of the Animal Care and Use Committee of Florida Internal University.

Results

Rhodopsin imaging of rat retina was performed with the pulsed SLO by acquiring the retinal images first under dark adaptation and then under light adaptation. In the *in vivo* imaging experiments a raster scan pattern consisting of 256 (horizontal) ×256 (vertical) scanning positions was used. The pulse repetition rate of the laser was 20 kHz. With the guidance of the NIR-SLO the dark adapted eye was imaged first. Then the room light was turned on immediately and a flashlight was also used to illuminate the eye to guarantee complete photo bleaching of the rod photoreceptors. After 20 seconds light adaptation, the second fundus image was acquired. *Figure 2* shows the experimental results. *Figure 2A* and *B* are fundus images acquired under dark adaptation and light adaptation, respectively. From the sharp edge of retinal vessels we are confident that the laser light was well focused on the retina. The central residual reflection from the cornea can still be observed and is labeled by the yellow arrow. *Figure 2C* shows the result calculated by using the following formula:

$$I_d = \left(I_{LA} - I_{DA}\right)/I_{LA} \qquad [1]$$

where I_d represents the normalized intensity difference between the light (I_{LA}) and dark (I_{DA}) adapted retinal images. From *Figure 2C* we can see that blood vessels and the optic disc appear black, which means at these areas light
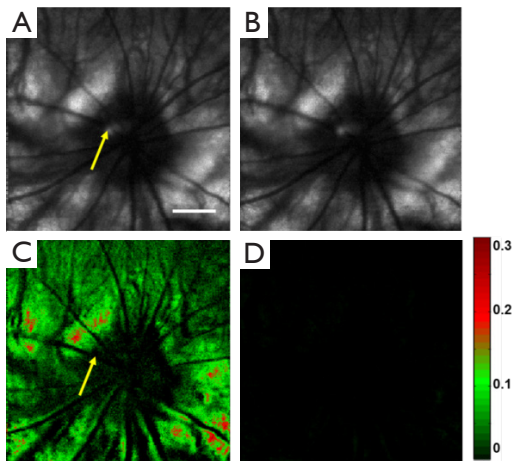
Figure 2 Rhodopsin imaging of a rat retina with external bleaching light between acquisition of the dark- and light- adapted images. (A) Retinal image of the dark-adapted retina; (B) retinal image of the light-adapted retina; (C) normalized differential image calculated from (A) and (B) representing the distribution of rhodopsin in the retina; (D) normalized differential image calculated from the two sequentially acquired light adapted images. Bar: 10°. (C) and (D) share the same color map.
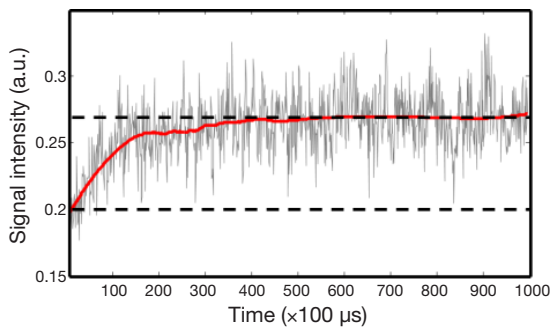

Figure 3 Time course of pulse train self-bleaching experiment. The two dashed lines represent the initial and the steady-state (bleached) signal intensity.

adaptation does not change the fundus reflection. This is reasonable because the retinal blood vessels are in front of the photoreceptors, which block the visible probing light from illuminating the photoreceptors, and there is no photoreceptor at the optic disc. Apart from the blood vessels and the optic disc, light reflection is increased in other areas of the retina due to photo bleaching of rhodopsin. The residual reflection from the cornea labeled in *Figure 2A* is eliminated in the differential image. The maximum signal increase is about 30%, which is close to the *ex vivo* data
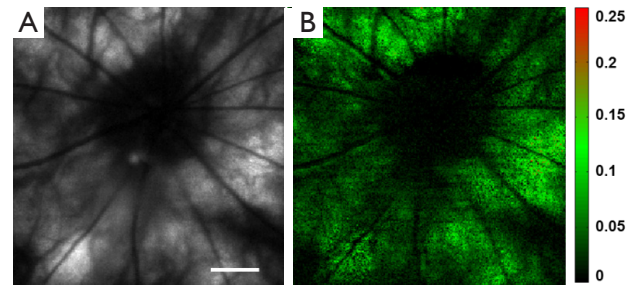

Figure 4 Results of rhodopsin bleaching in a rat retina by the probing light pulse with a pulse energy of 3 nJ and 45 s waiting time. (A) First retinal image acquired with the probe light under dark adaptation; (B) normalized differential image from the sequentially captured two images. Bar: 10°.

reported before by other groups (17).

To prove that *Figure 2C* represents rhodopsin distribution in the retina, we also acquired an image after the image in *Figure 2B* was taken for the light adapted retina. We then calculated the intensity difference of these two images for the light adapted retina by using the following formula:

$$I_d = \left(I_{LA2} - I_{LA1}\right) / I_{LA2} \qquad [2]$$

where I_{LA2} and I_{LA1} are the intensities of the second and the first light adapted images, respectively. *Figure 2D* shows the calculated differential image. From *Figure 2D* we can see that the intensity of the differential image is close to zero, which proved that *Figure 2C* is the result of photo-bleaching of the photoreceptors, and thus represents the rhodopsin distribution in the retina.

We examined the dynamic bleaching process of the rod photoreceptors by recording the reflected light signals from a pulse train containing 1,000 pulses with a pulse repetition rate of 10 KHz delivered to the dark-adapted retina. All the light pulses were delivered to the same point of the retina. *Figure 3* shows the recorded signal amplitude *vs.* time. We can clearly see that the reflected photons increased exponentially over time at beginning and reached a plateau after exposed to about 400 light pulses, i.e., a total light exposure of 0.6 μJ.

We designed another experiment to further examine the time dependent rhodopsin bleaching process. The laser pulse energy was set to be 3 nJ. Under dark adaptation, we imaged the rat retina twice with a 45 second time delay. A differential image was calculated from these two images by using Eq. [2], which is shown in *Figure 4*. We can see from *Figure 4* that the photoreceptors were bleached to at least

50% by the probe light pulses of the first image.

important for human applications.

Discussion

The experiments have proved that ns pulse can be used for rhodopsin imaging with good image quality. Rhodopsin can be bleached with either the probe light for imaging or the room light with sufficient waiting time (20 s in our experiment). The experiments showed in *Figure 2* have successfully revealed the rhodopsin distribution in the rat retina.

The experiments also showed that sufficient exposure and long enough waiting time are both required for fully bleaching rhodopsin. The experimental results shown in *Figure 4* proved that rhodopsin in the rods can be noticeably bleached by a total exposure of only 3 nJ at 532 nm. In contrast, the experiment in *Figure 3* shows that an exposure of 0.6 μJ is required to fully bleach the rods. This looks contradictory at first glance. The major difference between the two experiments is the time delay. Considering the rhodopsin photo-cycle we believe the reason for the difference in the results of *Figures 3* and *4* is the absorption of the rhodopsin intermediates generated in the photo-cycle. In the pulse train experiment, the first 400 pulses were delivered in 40 ms. According to the experiment of *Figure 3*, we hypotheses that the first several pulses have activated photo isomerization for all the rhodopsin molecules. The reduction of absorption for the following laser pulses over time was caused by the shift of absorption spectrum of the intermediates. Thus, *Figure 3* should be related to the time course of rhodopsin photo-cycle.

To quantify rhodopsin concentration, retinal exposure to the probing light in the dark-adapted state needs to be in a level that only a negligible amount of rhodopsin is bleached. However, reducing the power (or pulse energy) of the probing light will reduce the signal-to-noise ratio (SNR), which will possibly reduce the accuracy of rhodopsin concentration calculation. According to our experiments we believe reducing the exposure time to at least the nanosecond level will be a solution.

Different from conventional CW SLO where the exposure time is inversely proportional to the scanning speed (imaging speed), the pulsed-light SLO decouples the light exposure time from imaging speed. In pulsed-light SLO, where each light pulse contributes to one pixel of the image, the exposure time is determined by the pulse width while the imaging speed is determined by the pulse repetition rate. As a result, to increase the imaging speed we need a laser with higher pulse repetition rate, which is

Conclusions

We have demonstrated the feasibility of using a nano-second pulsed-light SLO to map rhodopsin distribution in rat eye *in vivo*. By reducing the exposure time of the photoreceptors, the technique minimizes the effect of absorption of rhodopsin intermediates, which can improve the measurement accuracy of rhodopsin concentration in the rod photoreceptors.

Acknowledgements

References

1. Wang Q, Schoenlein RW, Peteanu LA, Mathies RA, Shank CV. Vibrationally coherent photochemistry in the femtosecond primary event of vision. Science 1994;266:422-4.
2. Lewis JW, Kliger DS. Absorption spectroscopy in studies of visual pigments: spectral and kinetic characterization of intermediates. Methods Enzymol 2000;315:164-78.
3. Menon ST, Han M, Sakmar TP. Rhodopsin: structural basis of molecular physiology. Physiol Rev 2001;81:1659-88.
4. Rushton WA. Apparatus for analysing the light reflected from the eye of the cat. J Physiol 1952;117:47P-48P.
5. Rushton WA, Campbell FW. Measurement of rhodopsin in the living human eye. Nature 1954;174:1096-7.
6. Hood C, Rushton WA. The Florida retinal densitometer. J Physiol 1971;217:213-29.
7. Bedggood P, Metha A. Variability in bleach kinetics and amount of photopigment between individual foveal cones. Invest Ophthalmol Vis Sci 2012;53:3673-81.
8. Kilbride PE, Read JS, Fishman GA, Fishman M. Determination of human cone pigment density difference spectra in spatially resolved regions of the fovea. Vision

68

Liu et al. Rhodopsin imaging in the photoreceptors

Res 1983;23:1341-50.

9. Kemp CM, Faulkner DJ, Jacobson SG. The distribution and kinetics of visual pigments in the cat retina. Invest Ophthalmol Vis Sci 1988;29:1056-65.

10. van Norren D, van de Kraats J. Imaging retinal densitometry with a confocal Scanning Laser Ophthalmoscope. Vision Res 1989;29:1825-30.

11. Elsner AE, Burns SA, Hughes GW, Webb RH. Reflectometry with a scanning laser ophthalmoscope. Appl Opt 1992;31:3697-710.

12. Morgan JI, Pugh EN Jr. Scanning laser ophthalmoscope measurement of local fundus reflectance and autofluorescence changes arising from rhodopsin bleaching and regeneration. Invest Ophthalmol Vis Sci 2013;54:2048-59.

13. Barlow HB. Dark and light adaptation: psychophysics.

In: Jameson D, Hurvich LM, eds. Handbook of sensory physiology. Volume VII. Fourth edition. Berlin: Springer, 1972:1-28.

14. Jiao S, Jiang M, Hu J, Fawzi A, Zhou Q, Shung KK, Puliafito CA, Zhang HF. Photoacoustic ophthalmoscopy for in vivo retinal imaging. Opt Express 2010;18:3967-72.

15. Behn D, Doke A, Racine J, Casanova C, Chemtob S, Lachapelle P. Dark adaptation is faster in pigmented than albino rats. Doc Ophthalmol 2003;106:153-9.

16. Liu X, Wang CH, Dai C, Camesa A, Zhang HF, Jiao S. Effect of contact lens on optical coherence tomography imaging of rodent retina. Curr Eye Res 2013;38:1235-40.

17. Williams TP, Webbers JP, Giordano L, Henderson RP. Distribution of photon absorption rates across the rat retina. J Physiol 1998;508:515-22.